EFFECTS OF HIGH PRESSURE OIL SEALS ON
THE ROTORDYNAMIC RESPONSE OF A CENTRIFUGAL COMPRESSOR

by

Thomas J. Cerwinske

Maintenance and Engineering Superintendent

W. Ed Nelson

Manager of Maintenance Services
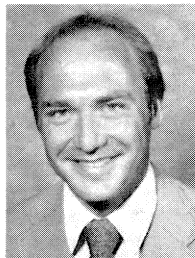
Amoco Oil Company

Texas City, Texas

and

Dana J. Salamone

President

Salamone Turbo Engineering, Incorporated

Houston, Texas

Thomas J. Cerwinske has been involved in the turbomachinery field since graduating from Iowa State University in 1976 with a B.S. degree in Mechanical Engineering. He is currently Maintenance and Engineering Superintendent of the Oil Movements Division for Amoco Oil Company's Texas City refinery in Texas City, Texas. He has served as Rotating Equipment Consultant and as a Rotating Equipment Engineer at the Amoco Texas City refinery as well as a Rotating Equipment Engineer at Amoco's headquarters in Chicago. He is a past Vice-President and Secretary-Treasurer of the Galveston County Chapter of the Texas Society of Professional Engineers. He is a member of the Texas Society of Professional Engineers, ASME, Tau Beta Pi, Pi Tau Sigma, and the Pump Symposium Advisory Committee.

W. Ed Nelson is the Manager of Maintenance Services for Amoco Oil Company in Texas City, Texas. His responsibilities include refinery instrument, electrical and machinery repair, as well as mobile equipment operation, and maintenance training.

Mr. Nelson graduated with a B.S. degree in Mechanical Engineering from Texas A&M University in 1951. He has spent 32 years in various engineering, materials management, and maintenance positions in Amoco's Texas City refinery. He is a member of ASME and the International Maintenance Institute. He is also a registered professional engineer in the State of Texas.

Mr. Nelson has authored several technical articles and is a noted speaker at seminars and technical meetings. He is also listed in several editions of Who's Who in the Southwest *and* World's Who in Commerce and Industry. *He is a member of the Turbomachinery Symposium Advisory Committee.*

Dana J. Salamone received his B.S. degree in Mechanical Engineering (1974) and his M.S. degree in Applied Mechanics (1977), both from the University of Virginia. He also earned a Master's degree in Business Administration from Houston Baptist University (1984).

He spent the first three years of his engineering career at Babcock and Wilcox in Lynchburg, Virginia, where he was responsible for seismic structural design, stress analysis and rotordynamics analysis. Then he spent two years as a project engineer in the Compressor Division of Allis-Chalmers Corporation in Milwaukee, Wisconsin. He was responsible for rotordynamics analysis of multi-stage centrifugal compressors and three dimensional (3-D) finite element stress analysis for horizontally-split fabricated casings.

For more than five years, Mr. Salamone was Chief Engineer for Centritech Corporation in Houston, Texas. In this capacity, he was responsible for rotordynamics analysis and bearing design consultation on industrial turbomachinery for the solution of vibration problems.

In 1984, Mr. Salamone founded Salamone Turbo Engineering, Incorporated. Turbo is an engineering consulting company that provides services in rotordynamics analysis and bearing design consultation for the solution of turbomachinery vibration problems in the utility, petroleum and chemical industries.

Mr. Salamone is a member of ASLE, ASME, NSPE, Society of Sigma Xi, and the Vibration Institute. He is also a registered professional engineer in the State of Texas.

ABSTRACT

The influence of high pressure bushing-type oil seals on the rotordynamic characteristics of a centrifugal gas compressor, which compresses hydrogen from 1700 psi to 1800 psi is discussed. The compressor rotor is driven through a gear coupling by a 10000 hp steam turbine, which has a governor speed range of 7900 cpm to 8850 cpm. This machine has had a long history of exhibiting high synchronous vibration under certain operating conditions.

A computer simulation identified that this rotor system can operate as two entirely different systems, which correlates well with field observations. The first system corresponds to the "normal" operating condition, where the bearings support the rotor and the oil seal bushings operate near the "centered" position. The second system corresponds to the condition where the seals carry the rotor weight and unload the bearings. This allows a level of flexibility to be introduced under the bearings, which reduces the effective damping. These rotor support changes shift the second critical speed into the operating speed range, which produces the high synchronous vibrations. In addition, the analysis indicates that the rotor is unstable in the condition where the seals support the rotor and where flexibility is introduced under the unloaded bearings.

INTRODUCTION

The effects of high pressure oil seals on the dynamic response of a recycle gas compressor are presented. This unit, shown in Figure 1, is driven by a 10000 hp steam turbine to compress hydrogen gas from 1700 psi to 1800 psi. The governor speed range is 7900 cpm to 8850 cpm. For purposes of discussion, 8400 cpm will be considered the operating speed.
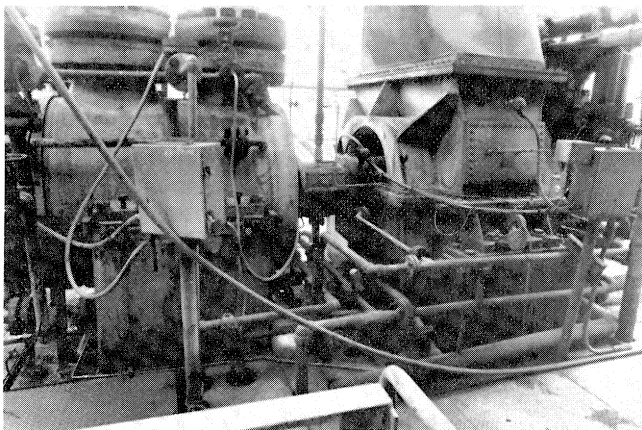

Figure 1. Recycle Gas Compressor.

The present system consists of a 557 lb rotor with a overall length of 63.09 in. The shaft is supported by two five-shoe tilting pad bearings separated by a 50.06 in span. The journal diameters are 4.0 in and 4.5 in on the thrust and coupling ends, respectively.

The process gas seals, located just inboard of the bearings on each end of the case, are high pressure bushing seals. Each seal consists of two floating bushing elements with a five mil to six mil clearance. The shaft diameter at the seals is 5.5 in. Therefore, if these seals lock up, they will behave similarly to plain journal bearings with external pressurization. These influences change the dynamic characteristics of the system.

This machine has had a history of exhibiting unpredictable, high vibration at synchronous speed, which has caused several serious wrecks. The magnitude of damage that has resulted from high vibration levels on this machine is demonstrated in Figures 2, 3, 4, and 5. Because of its importance to production, the reliability of this compressor is a necessity. A rotordynamics analysis was performed to determine the effect of high pressure oil seals on the dynamic characteristics of the compressor and to identify corrections that would improve the system vibration characteristics.

DESCRIPTION OF PRESENT ROTOR SYSTEM

The assembled compressor rotor (Figure 6), consists of a 63.09 in long shaft and two closed-disk impeller wheels. The com-
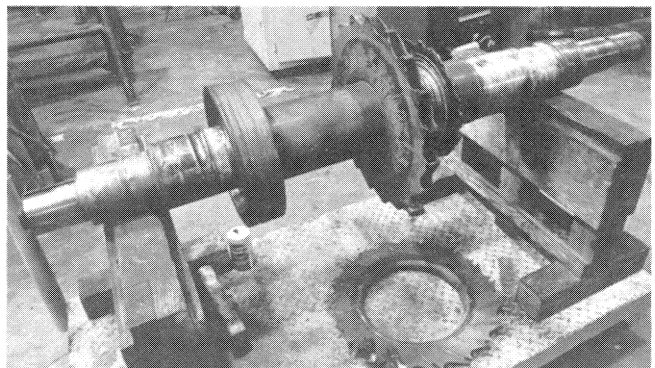

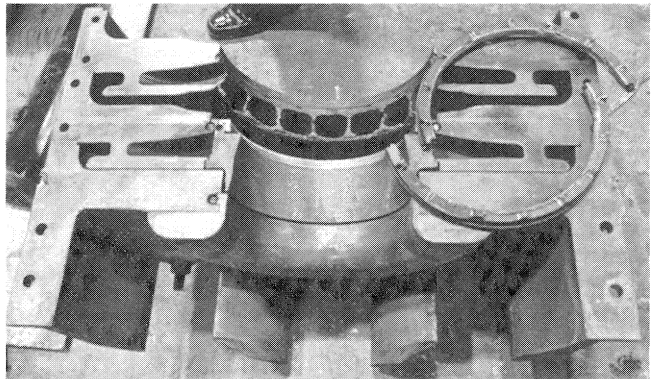Figure 2. Typical Rotor Wreck.

Figure 3. Stationary Bundle Damage Resulting from Wreck.
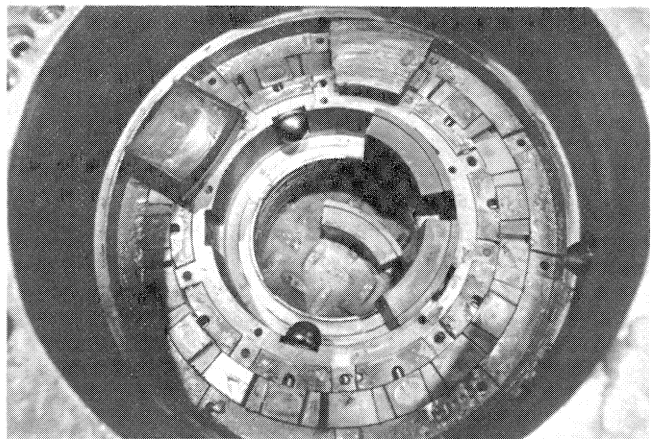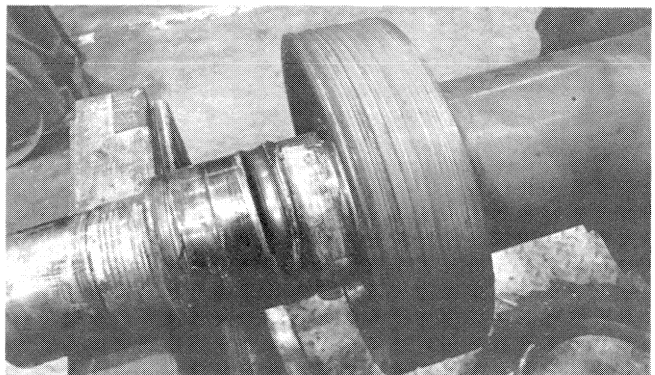

Figure 4. Bearing Damage Resulting from Wreck.

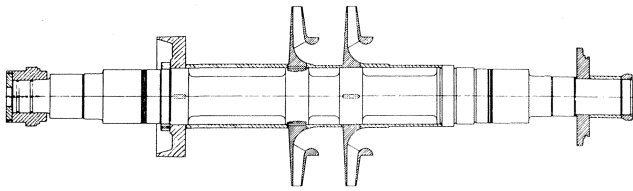Figure 5. Rotor Damage Resulting from Wreck.

Figure 6. Recycle Gas Compressor Rotor.

pressor is supported by two five-shoe tilting pad bearings. The journal diameters are 4.0 in and 4.5 in at the thrust end and coupling end, respectively. The computer model of the rotor is illustrated in Figure 7.

The rotor assembly is modelled as a series of shaft sections. The division lines indicate lumped mass stations containing the weight and inertia properties of the compressor wheels, balance piston, coupling, thrust collar, etc. The rotor model also includes the effect of the bearing fluid film stiffness and damping properties.
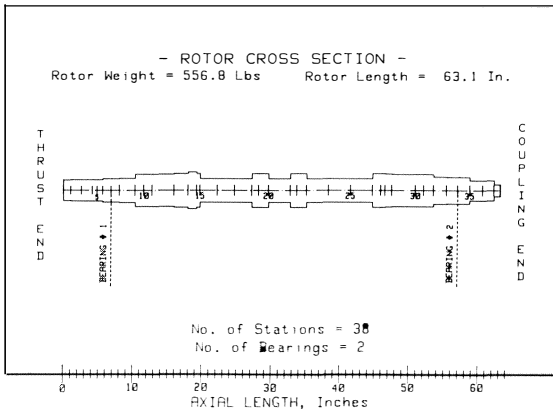

Figure 7. Computer Model of Compressor Rotor.

UNDAMPED CRITICAL SPEEDS

Critical Speed Map

The critical speed map is a plot of the first three undamped critical speeds vs a range of bearing stiffness values. The critical speeds increase as the bearing stiffness is increased up to a limit. Beyond this limit, the critical speeds are insensitive to increasing bearing stiffness, because the bearings are rigid relative to the rotor. Therefore, in the rigid region, the bearing damping is not effective for the suppression of vibration [1]. The critical speed map for the present rotor, with the existing coupling, is shown in Figure 8. For this rotor, the first critical speed has a rigid bearing limit of 5140 cpm.

Mode Shapes

The rotor mode shapes indicate the relative shape of the deflected rotor at the critical speeds. The mode shape also indicates the amount of motion at the bearing locations. The first two undamped critical speed mode shapes for the rotor considering stiffnesses of 5×10^5 lb/in at each bearing are presented in Figures 9 and 10.

EXISTING BEARINGS

Description

The rotor is supported in a pair of five-shoe tilting pad bearings, as illustrated in Figure 11. The thrust-end bearing has
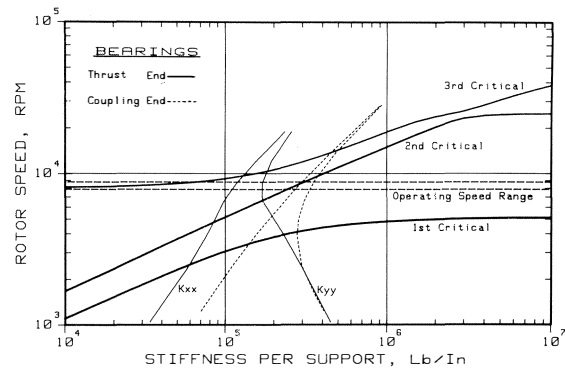

Figure 8. Undamped Critical Speed Map of Recycle Gas Compressor Supported on Journal Bearings Only. Oil seal bushings not considered.
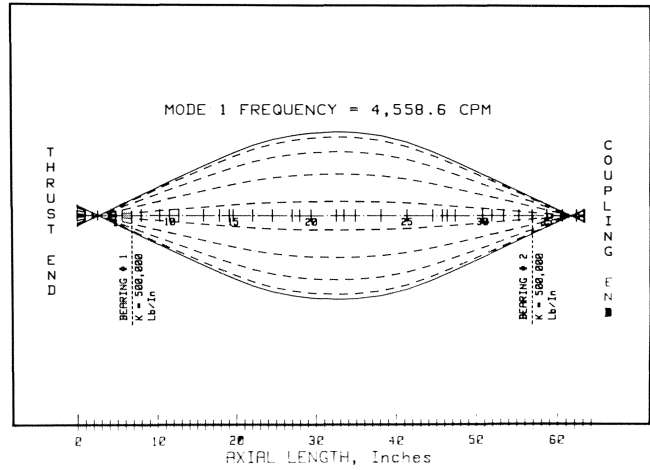
Figure 9. Mode Shape at First Undamped Critical Speed (4559 CPM) for Rotor Supported on Journal Bearings Only (Kb = 5 × 10^5 LB/IN). Oil seal bushings not considered.
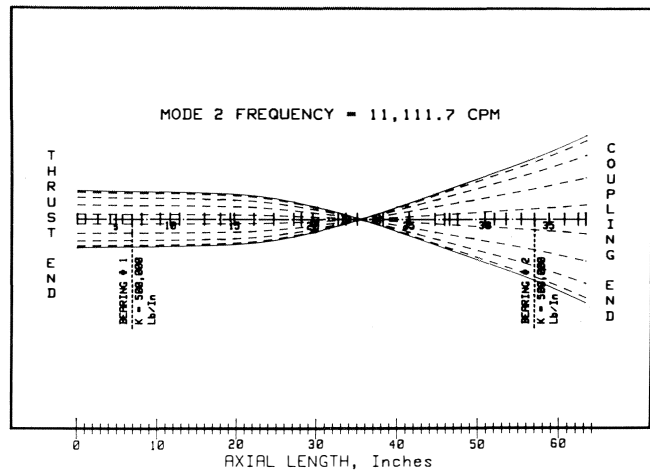
Figure 10. Mode Shape at Second Undamped Critical Speed (11112 CPM) for Rotor Supported on Journal Bearings Only (Kb = 5 × 10^5 LB/IN). Oil seal bushings not considered.

a diameter of 4.0 in, pad length of 1.62 in, diametral set clearance of 0.006 in, and preload of 0.143. The coupling-end bearing has a diameter of 4.5 in, pad length of 1.875 in, diametral set clearance of 0.006 in, and preload of 0.25. Both bearings are oriented with load on pad.
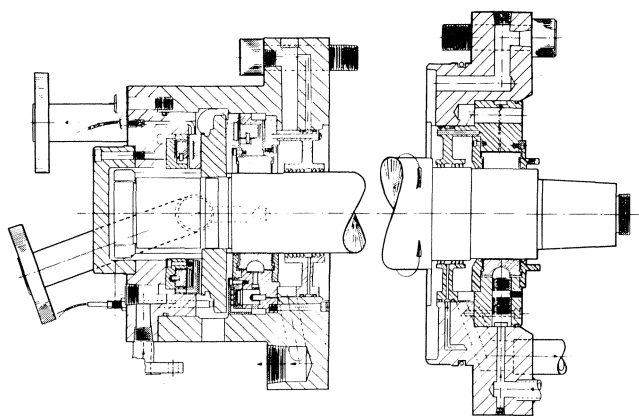
Figure 11. Recycle Gas Compressor Bearing Arrangement.

The existing oil is an International Standards Organization (ISO) 46, which is rated at 210 Saybolt Seconds Universal (SSU) at 100°F. This oil has an absolute viscosity of 1.93 microreyns at 150°F.

Bearing Coefficients

The stiffness and damping coefficients *vs* rotor speed for the thrust-end and coupling-end journal bearings, respectively, are shown in Figures 12 and 13. These coefficients represent the predicted properties for the bearings in the present condition with normal gravity loading. The bearing stiffnesses are cross-plotted on the map shown in Figure 8. The stiffness values for these bearings intersect the second mode curves very close to the operating speed (8400 cpm). These intersections, which are the undamped critical speeds, are listed in Table 1. Note that the running speed lies in the range listed for the second critical.
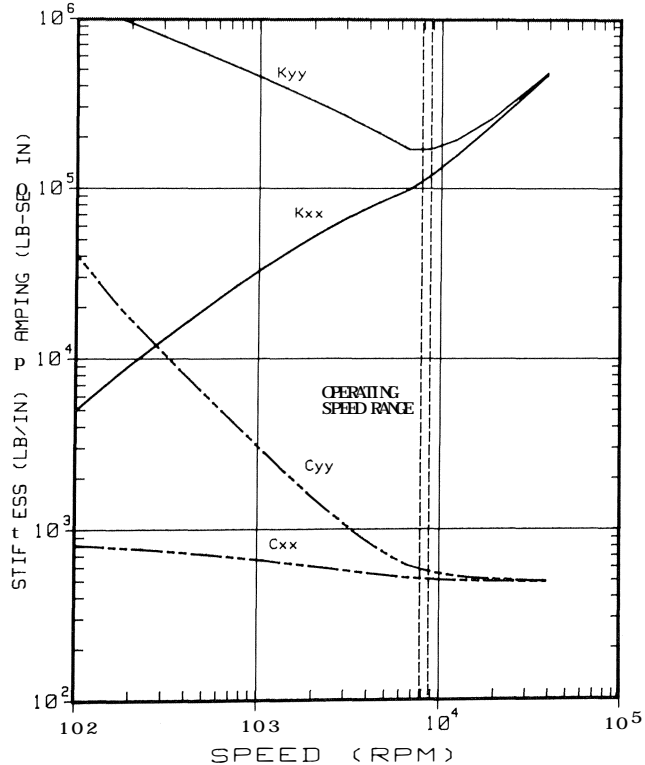
Figure 12. Thrust-end Bearing Stiffness and Damping Coefficients vs Speed.
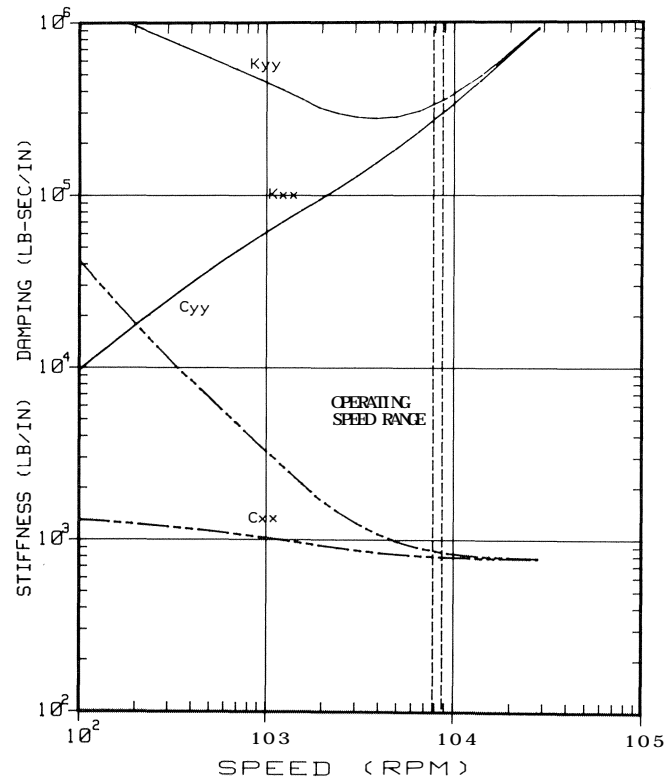
Figure 13. Coupling-end Bearing Stiffness and Damping Coefficients vs Speed.

Table 1. Undamped Critical Speeds of Compressor Supported in Journal Bearings Only. Oil seal bushings not considered.

|	Horizontal Plane	Vertical Plane
First Critical	Between 2,500 and 3,450 cpm	Between 3,900 and 4,100 cpm
Second Critical	Between 4,700 and 8,700 cpm	Between 6,900 and 9,800 cpm
Third Critical	Between 9,800 and 13,200 cpm	Between 10,600 and 13,900 cpm

Unloaded Bearing Coefficients

The stiffness and damping for the existing tilt pad bearings for a special assumed loading condition are listed in Tables 2 and 3. In this special case, the journals are assumed to be centered in the bearings, which means that the bearings are unloaded. These special coefficients were used in the seal analysis, where the seals support the rotor.

Stiffness and Damping Ratios

The stiffness and damping ratios for the existing rotor/bearing system are presented in Table 4. Barrett, et al., presented these ratios [2], and they were discussed by Salamone [1, 3]. The stiffness ratio is very acceptable at 2.27. This is well below the optimum value of six or less [2]. The damping is also acceptable at 133 percent of optimum.

Table 2. Thrust-end, Five-shoe Tilting Pad Bearing Coefficients for Unloaded Condition.

	Speed (cpm)				
	3000	6000	8400	10800	14000
Stiffness (lb/in):					
KXX = KYY	8.401x10⁴	1.68x10⁵	2.352x10⁵	3.02x10⁵	3.92x10⁵
Damping (lb-sec/in):					
CXX = CYY	809.44	809.44	809.44	809.44	809.44
Eccentricity (DIM)	0	0	0	0	0

Bearing Parameters
D = 4.0 in
L/D = 0.41 (L = 1.62)
M = 0.143 (preload)
CD' = 0.006 in ——— set clearance
 1.5 mils/in.
CD = 0.007 in. mach. pad clearance
W = 0 lbs
$\mu = 1.93 \times 10^{-6}$ reyns
PAD ARC = 58.2°

Table 3. Coupling-end, Five-shoe Tilting Pad Bearing Coefficients for Unloaded Condition.

	Speed (cpm)				
	3000	6000	8400	10800	14000
Stiffness (lb/in):					
KXX = KYY	1.5x10⁵	3.0x10⁵	4.2x10⁵	5.403x10⁵	7.0x10⁵
Damping (lb-sec/in):					
CXX = CYY	1231.3	1231.3	1231.3	1231.3	1231.3
Eccentricity (DIM)	0	0	0	0	0

Bearing Parameters
D = 4.5 in
L/D = 0.42 (L = 1.875)
M = 0.25 (preload)
CD' = 0.006 in ——— set clearance
 1.33 mils/in.
CD = 0.008 in. mach. pad clearance
W = 0 lb
$\mu = 1.93 \times 10^{-6}$ reyns
PAD ARC = 58.4°

Table 4. Stiffness and Damping Ratios for Compressor Supported in Tilting Pad Journal Bearings.

$W_{ROTOR} = 556.88$ lb $(M_m = 0.721)$
$N_{cr} = 5,140$ cpm $(\omega_{cr} = 538.26)$
$K_s = 2.09 \times 10^5$ lb/in
$C_{cr} = 776.17$ lb-sec/in

Bearing Coefficients at 5,100 cpm:
Thrust Kyy = 1.9x10⁵   Cyy = 725.7
Coupling Kyy = 2.85x10⁵   Cyy = 974.6
Stiffness Ratio: $\bar{K} = 2.27$
Optimum Damping Ratio: $\xi_{opt} = 1.64$
Actual Damping Ratio: $\xi_{act} = 2.19$
                                  $= 133\% \; \xi_{opt}$

FLOATING BUSHING SEALS

Description

The floating ring bushing oil seal arrangement on each end of the compressor is illustrated in Figure 14. Each seal consists of two floating bushings. High pressure oil at 1710 psi is supplied between the two bushings to provide an oil barrier against process gas leakage. The pressure distributions on each bushing are illustrated in Figures 15 and 16. The inboard side of this seal is exposed to approximately 1700 psi gas. The outboard side is atmospheric pressure.

A complete similation of this oil seal configuration would require a complex non-linear analysis. However, with a few simplifying assumptions, the seal effect can be approximated in order to assess the potential influence on the system dynamics. Specifically, a calculation can be made of the unbalanced pressure forces on these floating bushings in the high pressure environment. These forces can then be used to estimate an order of magnitude of the friction force on the sliding faces. It should be emphasized that this a very basic approximation, and

NOTE: OB = OUTBOARD BUSHING
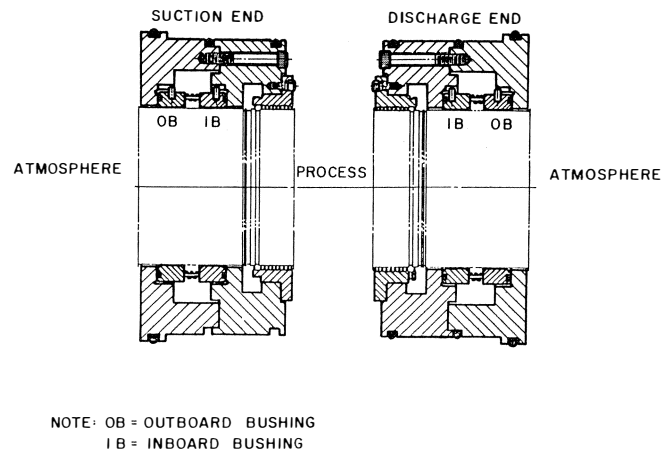   IB = INBOARD BUSHING

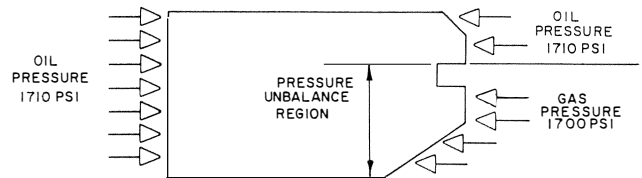Figure 14. Floating Bushing Oil Seal Arrangement.

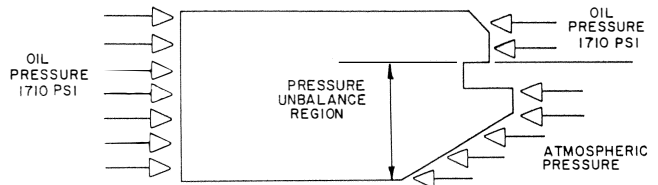Figure 15. Pressure Distribution on Inner Oil Seal Bushing.

Figure 16. Pressure Distribution on Outer Oil Seal Bushing.

that the actual seal exhibits a combination of hydrodynamic squeeze film and sliding friction behavior. This analysis assumes two approximations for the seal effect due to the hydrodynamic action only. These approximations will be discussed in more detail later.

As shown in Figure 15, the inboard bushing is exposed to 1700 psi gas pressure on the sliding face below the O-ring and 1710 psi oil on the other face. This yields a net unbalance pressure differential that would be approximately ten psi. The outboard bushing, shown in Figure 16, is exposed to 1710 psi oil along the free face and atmospheric pressure on the sliding face below the O-ring. Therefore, this bushing has an axial pressure differential of approximately 1710 psi. The unbalanced region between the top of the O-ring groove and the bore has an area of approximately 8.06 square in. Thus, the net force between this bushing and the support housing is 13787 lb. If hard-steel on hard-steel (greasy) is assumed, the static friction coefficient is 0.11. This should yield a static friction force of approximately 1517 lb, which is 2.6 times the rotor weight. Therefore, the seals can lock up and support enough load to unload the bearings.

The stationary vertical sliding face of the seal cans showed significant fretting damage (Figure 17). These damaged faces can increase the potential for seal lockup. Therefore, the seal cans were modified to accommodate a detonation-gun, tungsten carbide coating on these stationary sliding faces.
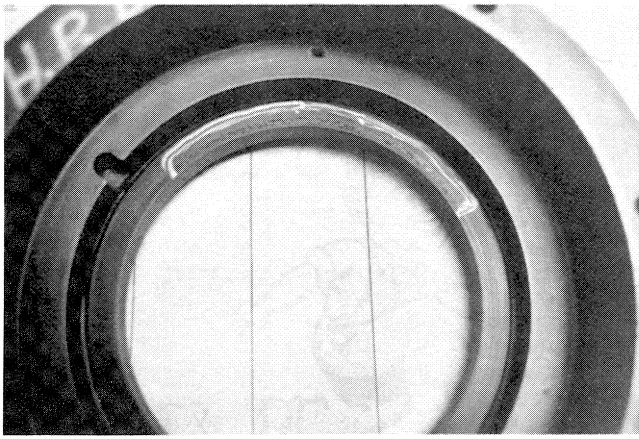
Figure 17. Oil Seal Cans Showing Damaged Vertical Sliding Face.

Oil Seal Stiffness and Damping Coefficients

The load capacity as a function of the eccentricity curve for the outboard bushing with an external pressure drop of 1710 psi for five different operating speeds is shown in Figure 18. The bushing diametral clearance is 0.005 in. Therefore, in the locked condition, this seal would have characteristics similar to a plain journal bearing with external pressurization. From a static point of view, the bushing is not capable of generating more load capacity than can be held by the friction force. This means that the load eccentricity curve ends at a 1517 lb load, for this approximation. At loads above this static friction force, the seal would slide, because the friction force would be exceeded. Consequently, the seal would move to another position. However, in this case, the friction force is several times the rotor weight, so it would be difficult for the rotor to exceed it.
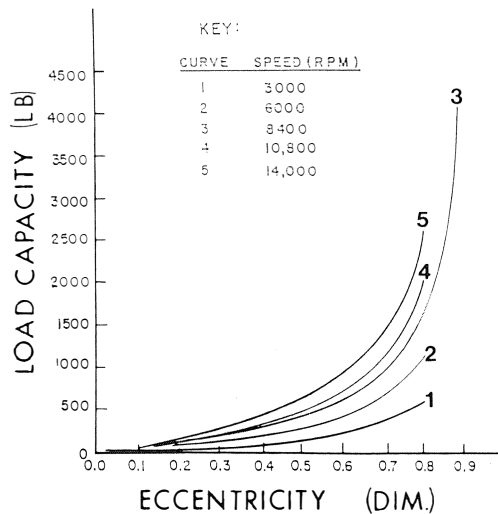

Figure 18. Load vs Eccentricity Curve for Outer Oil Seal Bushing with 0.005 IN Diametral Clearance and 1710 PSI Pressure Drop.

Two extreme conditions were assumed to assess the seal effects. In case one, it is assumed that the seal is centered, and therefore, carries no load (but still contributes stiffness and damping). In case two, it is assumed that the seals are supporting the entire shaft load, so that the tilt pad bearings become unloaded.

Tabulations of the stiffness and damping coefficients for differing operating speeds for the outer seal bushing previously described are reflected in Tables 5, 6 and 7. Note that the bushing journal has a diameter of 5.5 in, and the length-to-diamter (L/D) ratio of the bushing is 0.13. For Table 5, a centered outer bushing seal is assumed. Seal loads equal to the gravity loads are assumed in Tables 6 and 7. Note that the seal generates high cross-coupling, which could contribute a rotor destabilizing influence. In addition, the principle stiffness and damping introduce the effect of additional bearings into the overall system dynamics.

Table 5. Stiffness and Damping Coefficients for Unloaded (Centered) Thrust-end and Coupling-end Outer Oil Seal Bushings.

	Speed (cpm)				
	3000	6000	8400	10800	14000
Stiffness (lb/in):					
KXX	6.79×10^4	6.79×10^4	6.79×10^4	6.8×10^4	7.0×10^4
KXY	7.19×10^4	1.44×10^5	2.02×10^5	2.59×10^5	3.35×10^5
KYX	-7.19×10^4	-1.44×10^5	-2.02×10^5	-2.59×10^5	-3.35×10^5
KYY	6.79×10^4	6.79×10^4	6.79×10^4	6.8×10^4	7.0×10^4
Damping (lb-sec/in):					
CXX	4.58×10^2	4.58×10^2	4.58×10^2	4.58×10^2	4.57×10^2
CXY	0	0	0	0	0
CYX	0	0	0	0	0
CYY	4.58×10^2	4.58×10^2	4.58×10^2	4.58×10^2	4.57×10^2
Eccentricity (DIM)	0.0	0.0	0.0	0.0	0.0

Seal Parameters
D = 5.5 in
L/D = 0.13 (L = 0.73)
$CD = \dfrac{0.005 \text{ in}}{\text{mils/in.}}$ set clearance
W = 0 lbs
$\mu = 1.93 \times 10^{-6}$ reyns
$\rho = 8.09 \times 10^{-5}$
$\Delta P = 1710$ psi

Table 6. Stiffness and Damping Coefficients of Loaded Thrust-end Outer Oil Seal Bushing.

	Speed (cpm)				
	3000	6000	8400	10800	14000
Stiffness (lb/in):					
KXX	7.67×10^4	7.29×10^4	7.13×10^4	7.02×10^4	7.07×10^4
KXY	3.66×10^5	3.36×10^5	3.57×10^5	3.78×10^5	4.29×10^5
KYX	-1.37×10^5	-1.97×10^5	-2.47×10^5	-2.96×10^5	-3.65×10^5
KYY	9.28×10^4	8.22×10^4	7.78×10^4	7.45×10^4	7.37×10^4
Damping (lb-sec/in):					
CXX	8.71×10^2	6.26×10^2	5.62×10^2	5.23×10^2	4.98×10^2
CXY	0	0	0	0	0
CYX	0	0	0	0	0
CYY	2.37×10^3	1.07×10^3	8.04×10^2	6.57×10^2	5.71×10^2
Eccentricity	0.62	0.468	0.38	0.315	0.255
Minimum Film (MILS)					

Seal Parameters
D = 5.5 in
L/D = 0.13 (L = 0.73)
$CD' = \dfrac{0.005 \text{ in}}{\text{mils/in.}}$ set clearance
W = 243.5 lbs
$\mu = 1.93 \times 10^{-6}$ reyns
$\rho = 8.09 \times 10^{-5}$

Table 7. Stiffness and Damping Coefficients of Loaded Coupling-end Outer Oil Seal Bushing.

	Speed (cpm)				
	3000	6000	8400	10800	14000
Stiffness (lb/in):					
KXX	7.83×10^4	7.47×10^4	7.26×10^4	7.12×10^4	7.07×10^4
KXY	5.43×10^5	4.87×10^5	4.53×10^5	4.59×10^5	4.91×10^5
KYX	-1.64×10^5	-2.29×10^5	-2.71×10^5	-3.18×10^5	-3.83×10^5
KYY	9.69×10^4	8.73×10^4	8.13×10^4	7.76×10^4	7.48×10^4
Damping (lb-sec/in):					
CXX	1.04×10^3	7.29×10^2	6.17×10^2	5.62×10^2	5.22×10^2
CXY	0	0	0	0	0
CYX	0	0	0	0	0
CYY	3.54×10^3	1.56×10^3	1.03×10^3	8.02×10^2	6.59×10^2
Eccentricity (DIM)	0.68	0.545	0.45	0.38	0.31

Seal Parameters
D = 5.5 in
L/D = 0.13 (L = 0.73)
$CD' = \dfrac{0.005 \text{ in}}{\text{mils/in.}}$ set clearance
W = 313.4 lbs
$\mu = 1.13 \times 10^{-6}$ reyns
$\rho = 8.09 \times 10^{-5}$

Effect of Oil Seals on Critical Speeds

A comparison map showing the difference between supporting the shaft at the bearings and supporting it at the seals is shown in Figure 19. The dramatic change in the critical speeds when the seals act as load-carrying bearings is illustrated in this figure. Seal lock-up increases the first critical speed, but it decreases the second and third critical speeds. This is the same effect achieved by a bearing span reduction.
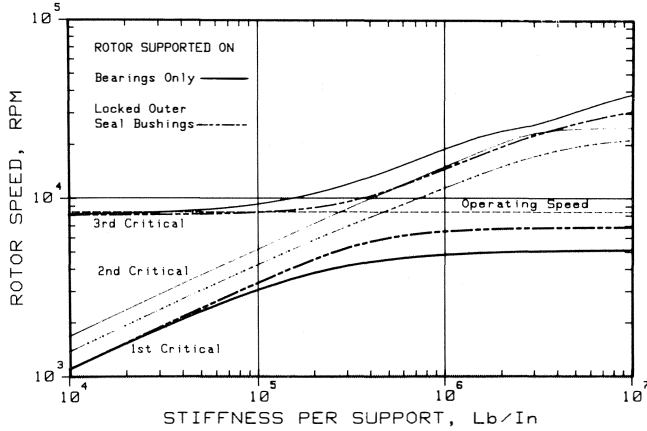

Figure 19. Undamped Critical Speed Map Showing Comparison Between Compressor Supported in Journal Bearings and Compressor Supported in Locked Outer Oil Seal Bushings.

The mode shapes corresponding to the rotor model, which assumes that the shaft is supported only by the outer oil seal bushings, are illustrated in Figures 20 and 21. Note that the figures indicate bearing locations at rotor stations 10 and 31, which are the seal locations. The original model (Figure 7) shows that the tilt pad bearings are located at stations 7 and 34. These mode shapes were plotted at an assumed seal bushing stiffness of 5×10^5 lb/in. The most important observation results from a comparison of Figures 10 and 21. Under normal conditions, with the bearings supporting the rotor, the undamped second critical speed is 11100 cpm. However, if the seals support the rotor, the second undamped critical speed drops to 8640 cpm. This observation warrants further investigation, which will be pursued in the unbalance response analysis.
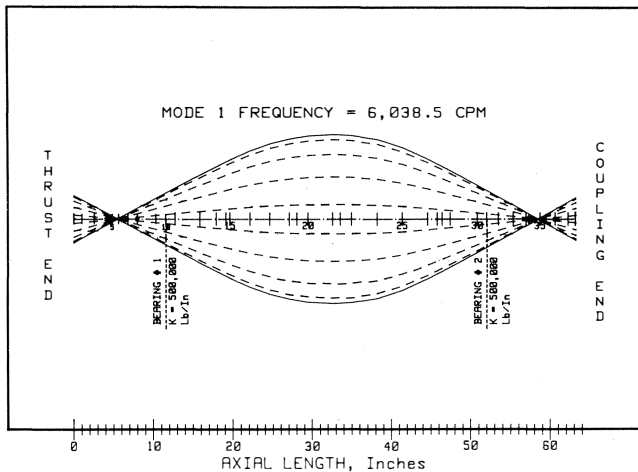

Figure 20. Mode Shape at First Undamped Critical Speed (6039 CPM) for Rotor Supported in Locked Outer Oil Seal Bushings Only (Kb = 5 × 10^5 LB/IN). Journal bearings not included.
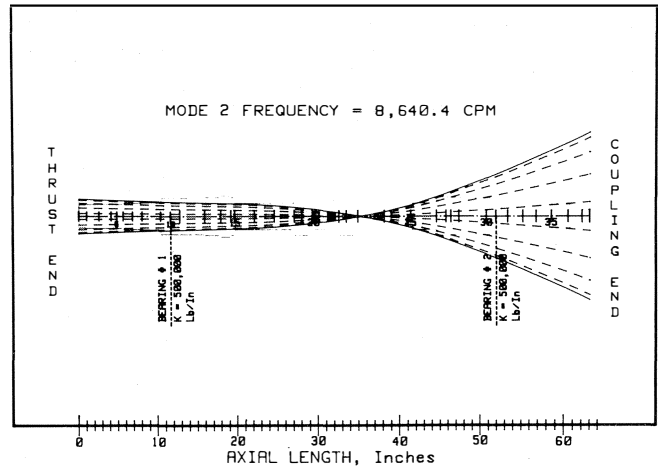

Figure 21. Mode Shape at Second Undamped Critical Speed (8640 CPM) for Rotor Supported Locked in Outer Oil Seal Bushings Only (Kb = 5 × 10^5 LB/IN). Journal bearings not included.

SYNCHRONOUS UNBALANCE RESPONSE

A synchronous unbalance response analysis simulates the rotor response due to unbalance [4, 5]. These results indicate the rotor sensitivity at the critical speeds, which reflects the effectiveness of the bearing damping.

Criteria

The rotor unbalance criteria used in this analysis consists of the following:
• In-Phase: ten percent of the rotor weight at the impeller wheels (at 90 degrees)
• Out-of-Phase couple at rotor ends:
  · ten percent of bearing No. 1 load at the thrust collar (at 0 degrees)
  · ten percent of bearing No. 2 load at the couping (at 180 degrees)
• Coupling: ten times the Navy standard-4W/N (at 180 degrees)
• Thrust collar: one mil eccentricity (at 0 degrees)

Summary of Results

The results of three configurations are presented in a series of tables, Bodé plots, and polar plots of the predicted synchronous unbalance response. The configurations consider different combinations of rotor support. The bearing characteristics for these special cases were presented previously. All of the amplitudes herein are equivalent to one-half peak-to-peak. These amplitudes should only be used for comparison purposes, since they are dependent on the assumed amount of unbalance. Unless specifically noted, these cases assume that the bearings and seals are supported by a rigid casing and base. The descriptions of the station numbers in the computer model are listed in Table 8.

Configuration 1

Configuration 1 represents the rotor response for the existing tilt pad bearings carrying all of the load with locked, centered outer oil seal bushings. The peak responses occur between 5400 cpm and 5550 cpm at all locations except the coupling end bearing and coupling, which have peaks betweeen 5700 cpm and 6300 cpm (Table 9). These peak response speeds correlate well with the first critical speed of 5400 cpm measured in the refinery. The response amplitudes at the running speed (8400

Table 8. Rotor Computer Model Station Location Cross Reference.

Station Number	Location
5	Thrust Collar
7	Thrust End Bearing
10	Outer Seal Bushing
19	First Stage Wheel
22	Second Stage Wheel
31	Outer Seal Bushing
34	Coupling End Bearing
37	Coupling

cpm) are presented in Table 10. The response plots for this case are presented in Figures 22, 23 and 24. The amplitude distribution along the shaft at running speed is shown in Figure 25.

Up to this point, the rotor model does not indicate peak responses near the running speed. However, under certain operating conditions, this machine periodically experiences high synchronous vibration. Specifically, it is believed that the seals lock up and alter the rotor/bearing system characteristics. It was previously reported that the magnitude of the outer bushing lockup forces could be several times the rotor weight. Therefore, the seals could act as bearings supporting the shaft. In addition, the undamped critical speed analysis results indicated that if the oil seals support the rotor, the second critical speed could decrease into the running speed range. Locked outer seal bushings carrying the shaft load are considered in configurations 2 and 3.

Configuration 2

The rotor response for the locked outer oil seal bushings carrying all of the rotor load is considered as configuration 2. In this case, the tilt pad bearings become unloaded, so that the centered journal assumption was used for the tilt pad stiffness and damping. In this case, the bearing pedestals are assumed to be rigid. Peak responses between 5550 cpm and 6300 cpm are shown in Table 11. However, there is still no response near the running speed. The rotor amplitudes at running speed are

Table 9. Synchronous Peak Response Amplitudes (Mils) for Compressor Configuration Number One—Considers Rotor Supported in Tilting Pad Journal Bearings with Rigid Pedestals. Effects of Locked, Unloaded (Centered) Outer Oil Seal Bushings also Included.

	Shaft Location							
	5	7	10	19	22	31	34	37
	Thrust Collar	Thrust End Bearing	Seal Thrust End	First Stage Wheel	Second Stage Wheel	Seal Coupling End	Coupling End Bearing	Coupling
First Peak								
Horizontal (X) Peak	0.30	0.28	0.33	0.79	0.82	0.25	0.10	0.33
Peak Speed	5400	5550	5550	5550	5550	5400	6300	6000
Vertical (Y) Peak	0.24	0.23	0.33	0.86	0.88	0.26	0.09	0.33
Peak Speed	5400	5400	5550	5550	5550	5400	6000	5700
Second Peak								
Horizontal (X) Peak	No Peak[1]	No Peak	No Peak	No Peak	No Peak	No Peak	No Peak	No Peak
Peak Speed	—	—	—	—	—	—	—	—
Vertical (Y) Peak	No Peak	No Peak	No Peak	No Peak	No Peak	No Peak	No Peak	No Peak
Peak Speed	—	—	—	—	—	—	—	—

[1] Note: No peak found up to 13950 cpm.

Table 10. Synchronous Response Amplitudes (Mils) at Running Speed (8,400 CPM) for Compressor Configuration Number One—Considers Rotor Supported in Tilting Pad Journal Bearings with Rigid Pedestals. Effects of locked, unloaded (centered) outer oil seal bushings also included.

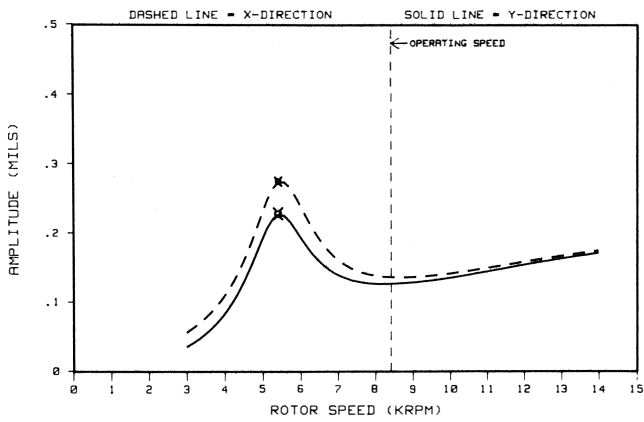|	Shaft Location							
	5	7	10	19	22	31	34	37
	Thrust Collar	Thrust End Bearing	Seal Thrust End	First Stage Wheel	Second Stage Wheel	Seal Coupling End	Coupling End Bearing	Coupling
Horizontal (X)	0.12	0.14	0.20	0.39	0.39	0.05	0.12	0.28
Vertical (Y)	0.10	0.13	0.20	0.39	0.38	0.05	0.11	0.27
% Change From Case Without Seals								
Horizontal (X)	−37	−30	−17	+11	+15	+67	+9	+12
Vertical (Y)	−38	−28	−13	+11	+12	+25	0	+8

+ = Increase

− = Decrease

Figure 22a. Synchronous Response Amplitudes vs Rotor Speed at Thrust-end Bearing Location for Compressor Configuration Number One—Considers Rotor Supported in Tilting Pad Journal Bearings with Rigid Pedestals. Effects of locked, unloaded (centered) outer oil seal bushings also included.
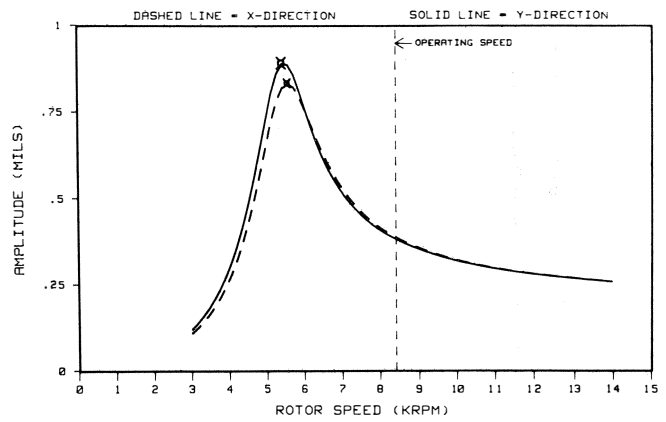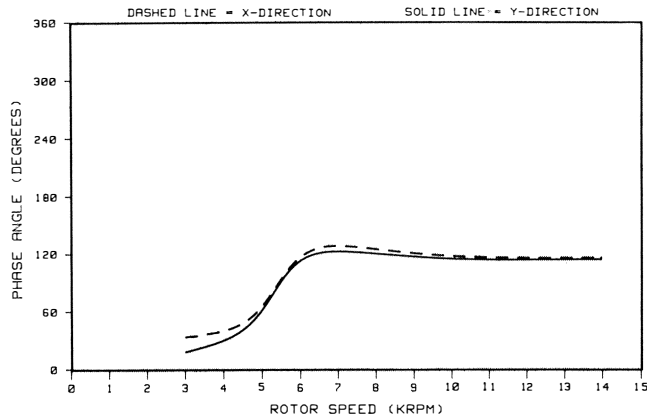

Figure 23a. Synchronous Response Amplitudes vs Rotor Speed at Second Stage Wheel Location (Near Rotor Center) for Compressor Configuration Number One—Considers Rotor Supported in Tilting Pad Journal Bearings with Rigid Pedestals. Effects of locked, unloaded (centered) outer oil seal bushings also included.

Figure 22b. Response Phase Angles vs Rotor Speed at Thrust-end Bearing Location for Compressor Configuration Number One.
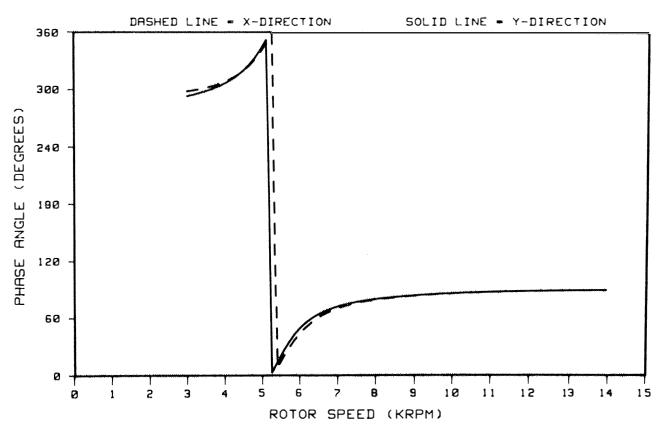

Figure 23b. Response Phase Angles vs Rotor Speed at Second Stage Wheel Location (Near Rotor Center) for Compressor Configuration Number One.
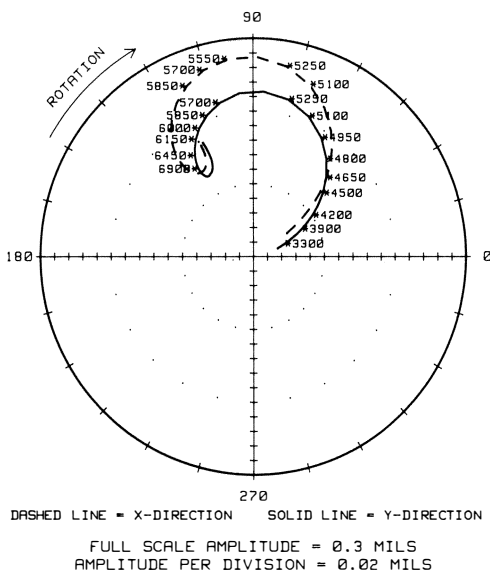

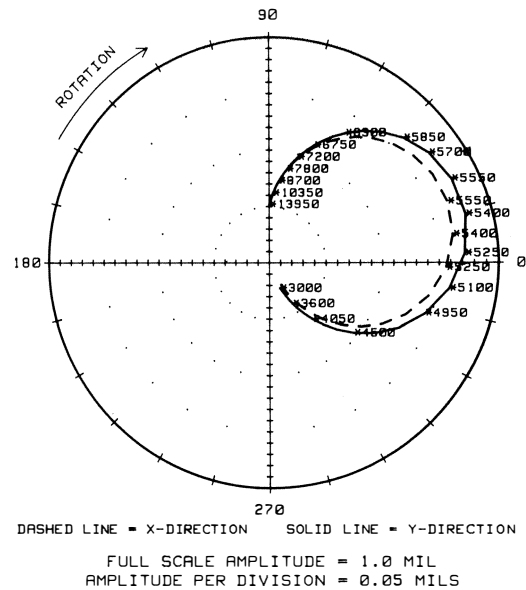Figure 22c. Nyquist Plot of Response at Thrust-end Bearing Location for Compressor Configuration Number One.

Figure 23c. Nyquist Plot of Response at Second Stage Wheel Location (Near Rotor Center) for Compressor Configuration Number One.
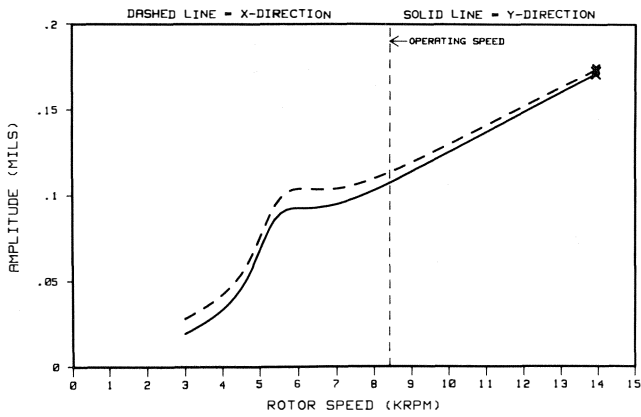
Figure 24a. Synchronous Response Amplitudes vs Rotor Speed at Coupling-end Bearing Location for Compressor Configuration Number One—Considers Rotor Supported in Tilting Pad Journal Bearings with Rigid Pedestals. Effects of locked, unloaded (centered) outer oil seal bushings also included.
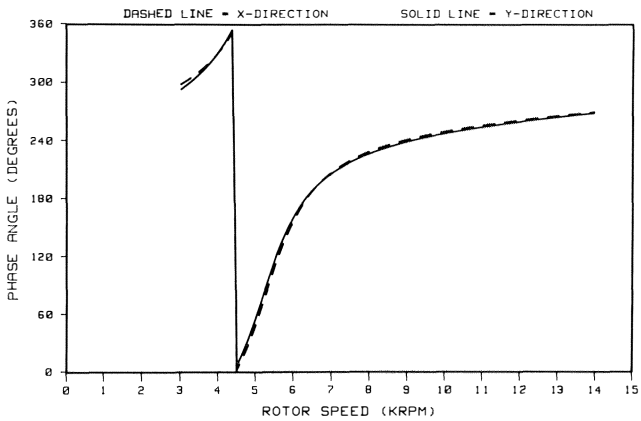

Figure 24b. Response Phase Angles vs Rotor Speed at Coupling-end Bearing Location for Compressor Configuration Number One.

DASHED LINE = X-DIRECTION   SOLID LINE = Y-DIRECTION

FULL SCALE AMPLITUDE = 0.2 MILS
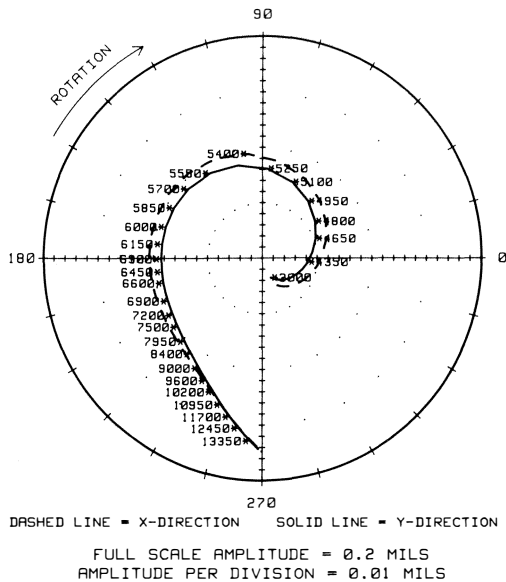AMPLITUDE PER DIVISION = 0.01 MILS

Figure 24c. Nyquist Plot of Response at Coupling-end Bearing Location for Compressor Configuration Number One.
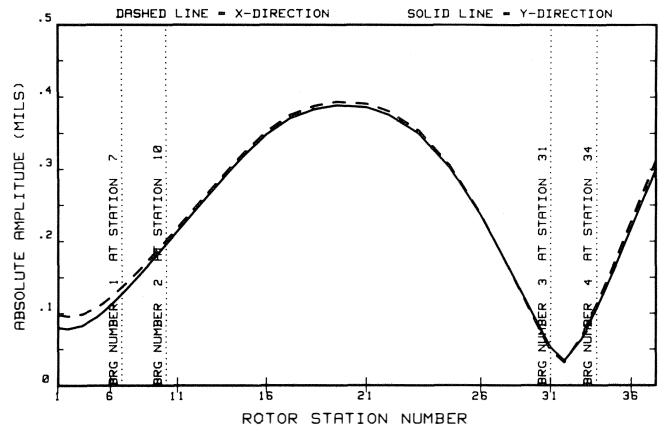

Figure 25. Magnitude of Synchronous Response Amplitude Vectors (Magnitude Only) Along Rotor Shaft at Running Speed (8400 CPM) for Compressor Configuration Number One.

presented in Table 12. The response plots are presented in Figures 26, 27, and 28. Response distribution along the rotor at the running speed is depicted in Figure 29.

Configuration 3

The rotor is supported in locked outer oil seal bushings in configuration 3. However, this case also assumes that the bearing support pedestals are flexible. The assumed pedestal stiffness was 1×10^5 lb/in in the horizontal and vertical directions at both bearings. Responses at 8550 cpm and 9600 cpm are shown in Table 13. This assumed system simulates the mechanism that could cause high vibration at the running speed. The amplitudes at the running speed are listed in Table 14. The response plots for this case are presented in Figures 30, 31, and 32. The rotor amplitude distribution at the running speed is presented in Figure 33.

ROTOR STABILITY

Rotor stability is assessed by calculating the damped eigenvalues of the rotor/bearing system [6, 7]. The damped eigenvalue is a complex number composed of a real part (λ), which is the growth factor and an imaginary part (ω_d), which is the damped natural frequency.

The log decrement (δ) is used to indicate the stability of a system. It represents the natural logarithm of the ratio of two successive amplitudes of system vibration, and is computed by the formula: $\delta = -2\pi\lambda/\omega_d$. If δ is positive, the system is stable. If δ is negative, the system is unstable. From experience, it is desirable to have a log decrement (δ) of $+0.25$ or greater.

Bearings Carry Rotor without Seal Effects

The log decrements for varying aerodynamic cross-coupling, assuming the tilt pad bearings carry the rotor and neglecting the oil seal effects, are listed in Table 15. Note that the rotor is stable in all cases. The logarithmic decrement is $+0.9$ with no aerodynamic cross-coupling. With 40592 lb/in of cross-coupling (beta = 8), the logarithmic decrement is reduced to $+0.2$. The "beta value" was introduced by Alford [8].

Bearings Carry Rotor with Locked Centered Oil Seals

The aerodynamic cross-coupling log decrements responses, assuming the tilt pad bearings support the rotor, are listed in Table 16. This case also includes the effects of locked outer oil seal bushings in the centered position. In all cases, the rotor is

Table 11. Synchronous Peak Response Amplitudes (Mils) for Compressor Configuration Number Two—Considers Rotor Supported in Locked, Outer Oil Seal Bushings with Rigid Pedestals. Also considers effects of unloaded (centered) tilting pad journal bearings on rigid pedestals.

| | Shaft Location | | | | | | | |
| | 5 | 7 | 10 | 19 | 22 | 31 | 34 | 37 |
	Thrust Collar	Thrust End Bearing	Seal Thrust End	First Stage Wheel	Second Stage Wheel	Seal Coupling End	Coupling End Bearing	Coupling
First Peak								
Horizontal (X) Peak	0.24	0.20	0.32	0.97	1.00	0.28	0.08	0.38
Peak Speed	5550	5550	5700	5700	5700	5700	5850	5850
Vertical (Y) Peak	0.19	0.16	0.20	0.63	0.65	0.15	0.10	0.33
Peak Speed	5850	5850	6150	6000	6000	5850	6600	6300
Second Peak								
Horizontal (X) Peak	No Peak[1]	No Peak	No Peak	No Peak	No Peak	No Peak	No Peak	No Peak
Peak Speed	—	—	—	—	—	—	—	—
Vertical (Y) Peak	No Peak	No Peak	No Peak	No Peak	No Peak	No Peak	No Peak	No Peak
Peak Speed	—	—	—	—	—	—	—	—

[1] Note: No peak found up to 13950 cpm.

Table 12. Synchronous Response Amplitudes (Mils) at Running Speed (8,400 CPM) for Compressor Configuration Number Two—Considers Rotor Supported in Locked, Outer Oil Seal Bushings with Rigid Pedestals. Also considers effects of unloaded (centered) tilting pad journal bearings on rigid pedestals.

| | Shaft Location | | | | | | | |
| | 5 | 7 | 10 | 19 | 22 | 31 | 34 | 37 |
	Thrust Collar	Thrust End Bearing	Seal Thrust End	First Stage Wheel	Second Stage Wheel	Seal Coupling End	Coupling End Bearing	Coupling
Horizontal (X)	0.06	0.09	0.17	0.39	0.39	0.07	0.08	0.23
Vertical (Y)	0.05	0.07	0.15	0.40	0.40	0.06	0.09	0.26
% Change From Case Without Seals								
Horizontal (X)	− 68	− 15	− 19	+ 11	+ 15	+ 133	− 27	− 8
Vertical (Y)	− 69	− 61	− 35	+ 14	+ 18	+ 50	− 18	+ 4

+ = Increase
− = Decrease
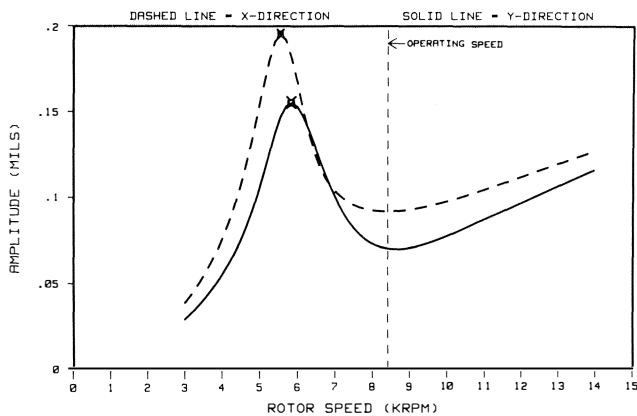
Figure 26a. Synchronous Response Amplitudes vs Rotor Speed at Thrust-end Bearing Location for Compressor Configuration Number Two—Considers Rotor Supported in Locked, Outer Oil Seal Bushings with Rigid Pedestals. Also considers effects of unloaded (centered) tilting pad journal bearings on rigid pedestals.
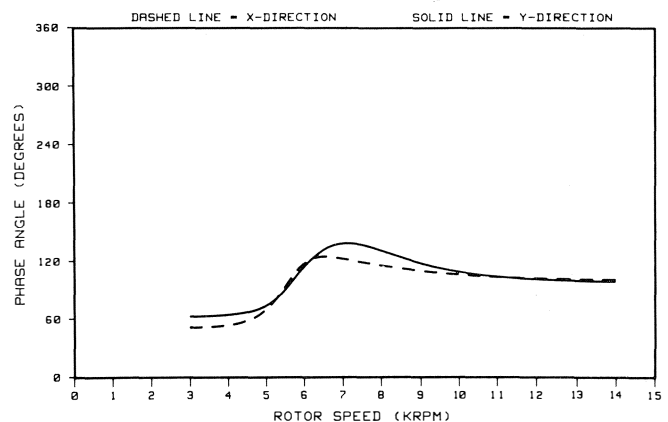

Figure 26b. Response Phase Angles vs Rotor Speed at Thrust-end Bearing Location for Compressor Configuration Number Two.
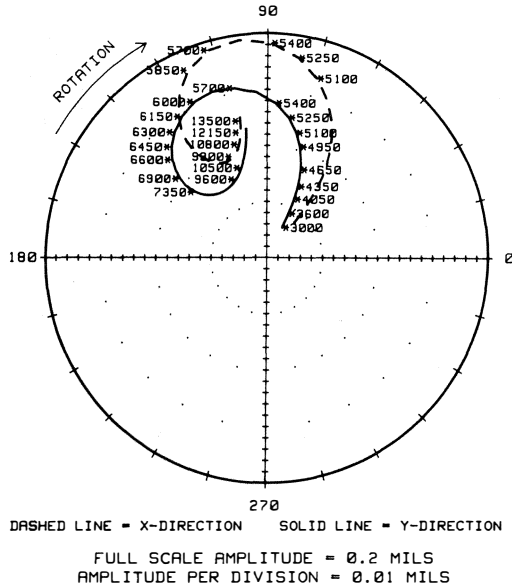
DASHED LINE = X-DIRECTION   SOLID LINE = Y-DIRECTION

FULL SCALE AMPLITUDE = 0.2 MILS
AMPLITUDE PER DIVISION = 0.01 MILS

Figure 26c. Nyquist Plot of Response at Thrust-end Bearing Location for Compressor Configuration Number Two.

DASHED LINE = X-DIRECTION   SOLID LINE = Y-DIRECTION

Figure 27a. Synchronous Response Amplitudes vs Rotor Speed at Second Stage Wheel Location (Near Rotor Center) for Compressor Configuration Number Two—Considers Rotor Supported in Locked, Outer Oil Seal Bushings with Rigid Pedestals. Also considers effects of unloaded (centered) tilting pad journal bearings on rigid pedestals.

DASHED LINE = X-DIRECTION   SOLID LINE = Y-DIRECTION

Figure 27b. Response Phase Angles vs Rotor Speed at Second Stage Wheel Location (Near Rotor Center) for Compressor Configuration Number Two.

DASHED LINE = X-DIRECTION   SOLID LINE = Y-DIRECTION

FULL SCALE AMPLITUDE = 1.0 MIL
AMPLITUDE PER DIVISION = 0.05 MILS

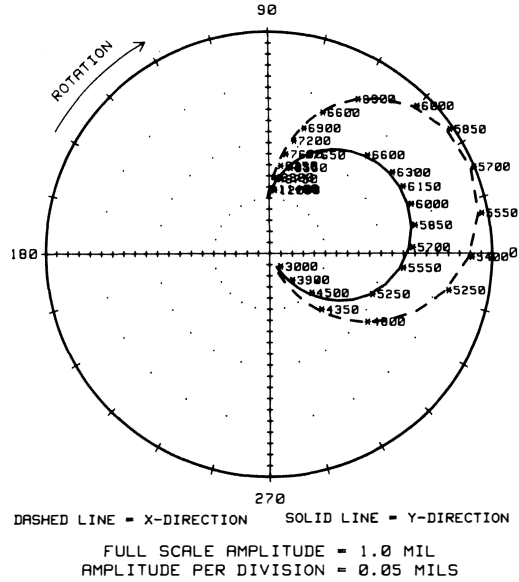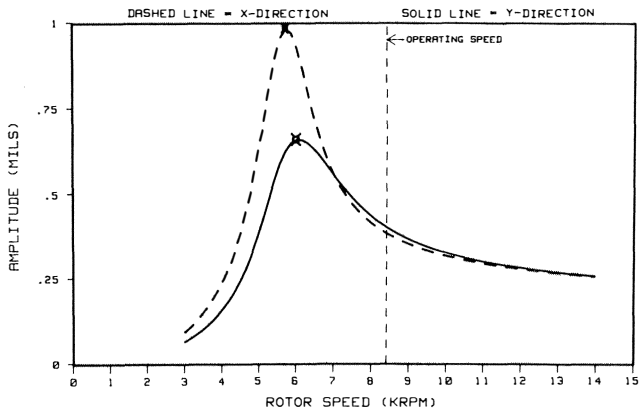*Figure 27c. Nyquist Plot of Response at Second Stage Wheel Location (Near Rotor Center) for Compressor Configuration Number Two.*

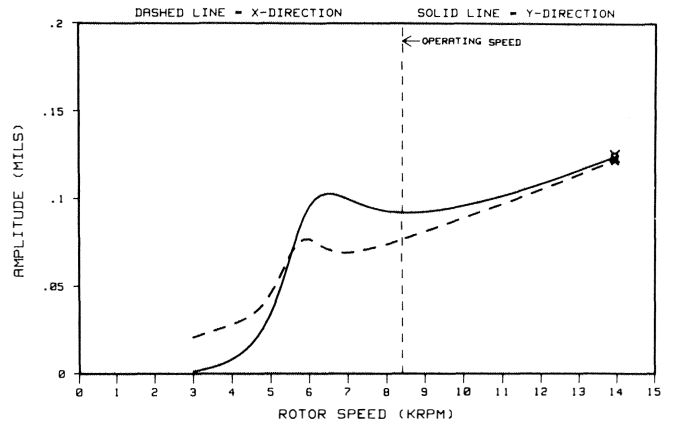DASHED LINE = X-DIRECTION   SOLID LINE = Y-DIRECTION

Figure 28a. Synchronous Response Amplitudes vs Rotor Speed at Coupling-end Bearing Location for Compressor Configuration Number Two—Considers Rotor Supported in Locked, Outer Oil Seal Bushings with Rigid Pedestals. Also considers effects of unloaded (centered) tilting pad journal bearings on rigid pedestals.
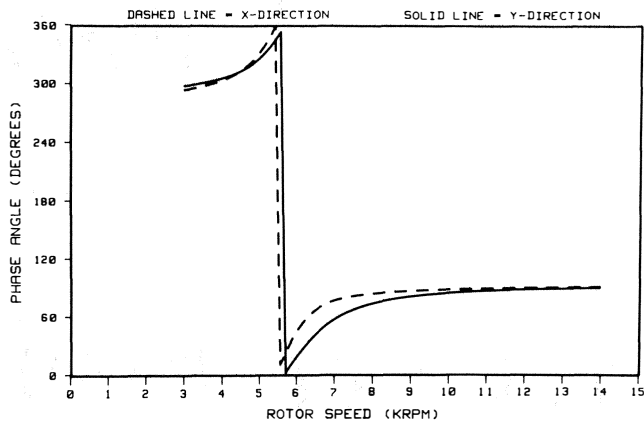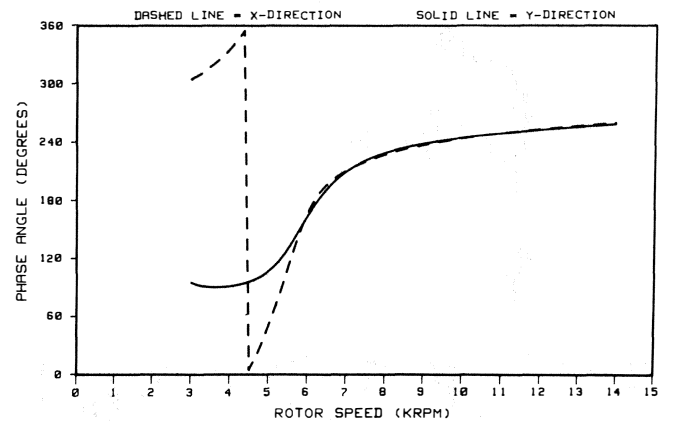

DASHED LINE = X-DIRECTION   SOLID LINE = Y-DIRECTION

Figure 28b. Response Phase Angles vs Rotor Speed at Coupling-end Bearing Location for Compressor Configuration Number Two.

DASHED LINE = X-DIRECTION   SOLID LINE = Y-DIRECTION

FULL SCALE AMPLITUDE = 0.1 MILS
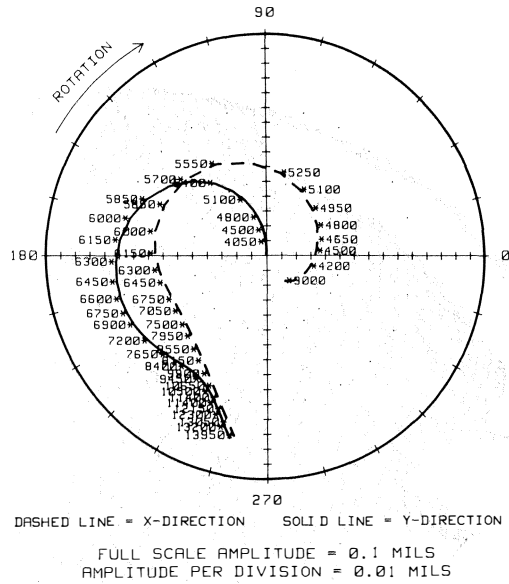AMPLITUDE PER DIVISION = 0.01 MILS

Figure 28c. Nyquist Plot of Response at Coupling-end Bearing Location for Compressor Configuration Number Two.
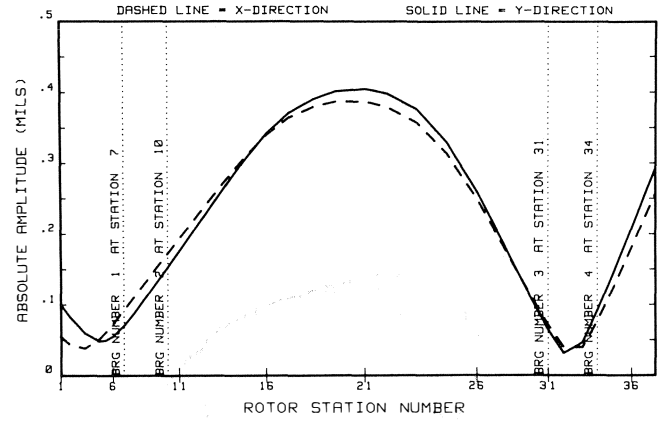

Figure 29. Magnitude of Synchronous Response Amplitude Vectors (Magnitude Only) Along Rotor Shaft at Running Speed (8400 CPM) for Compressor Configuration Number Two.

stable, but less stable than the case without seal effects. The logarithmic decrement with no aerodynamic cross-coupling is $+0.9$. The logarithmic decrement decreases to $+0.11$ with an aerodynamic loading of 40592 lb/in.

Table 13. Synchronous Peak Response Amplitudes (Mils) for Compressor Configuration Number Three—Considers Rotor Supported in Locked, Outer Oil Seal Bushings. Also considers effects of unloaded (centered) tilting pad journal bearings on flexible pedestals $(Kp = 1x10^5 \, lb/in)$.

				Shaft Location				
	5	7	10	19	22	31	34	37
	Thrust Collar	Thrust End Bearing	Seal Thrust End	First Stage Wheel	Second Stage Wheel	Seal Coupling End	Coupling End Bearing	Coupling
First Peak								
Horizontal (X) Peak	0.76	0.71	0.60	0.51	0.48	0.11	0.17	0.36
Peak Speed	7800	7800	7950	6150	6150	4650	6600	6450
Vertical (Y) Peak	0.58	0.52	0.44	0.75	0.76	0.06	0.34	0.70
Peak Speed	6750	6750	7050	7050	7050	5400	7200	7050
Second Peak								
Horizontal (X) Peak	No Peak[1]	No Peak	No Peak	0.48	0.45	No Peak	0.44	0.70
Peak Speed				8550	8550		9600	9300
Vertical (Y) Peak	No Peak	No Peak	No Peak	No Peak	No Peak	No Peak	0.38	0.66
Peak Speed							9450	9000

[1] Note: No peak found up to 13950 cpm.

Table 14. Synchronous Response Amplitudes (Mils) at Running Speed (8,400 CPM) for Compressor Configuration Number Three—Considers Rotor Supported in Locked, Outer Oil Seal Bushings. Also considers effects of unloaded (centered) tilting pad journal bearings on flexible pedestals $(Kp = 1x10^5 \, lb/in)$.

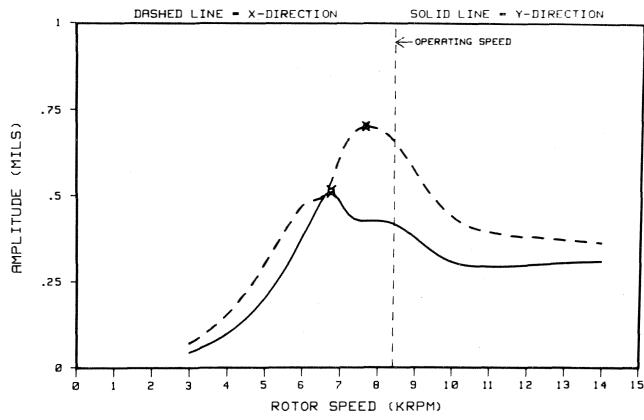|				Shaft Location				
	5	7	10	19	22	31	34	37
	Thrust Collar	Thrust End Bearing	Seal Thrust End	First Stage Wheel	Second Stage Wheel	Seal Coupling End	Coupling End Bearing	Coupling
Horizontal (X)	0.72	0.67	0.58	0.48	0.45	0.16	0.36	0.63
Vertical (Y)	0.45	0.43	0.41	0.53	0.51	0.11	0.36	0.65

Figure 30a. Synchronous Response Amplitudes vs Rotor Speed at Thrust-end Bearing Location for Compressor Configuration Number Three—Considers Rotor Supported in Locked, Outer Oil Seal Bushings. Also considers effects of unloaded (centered) tilting pad journal bearings on flexible pedestals (Kp = 1 × 10^5 lb/in).
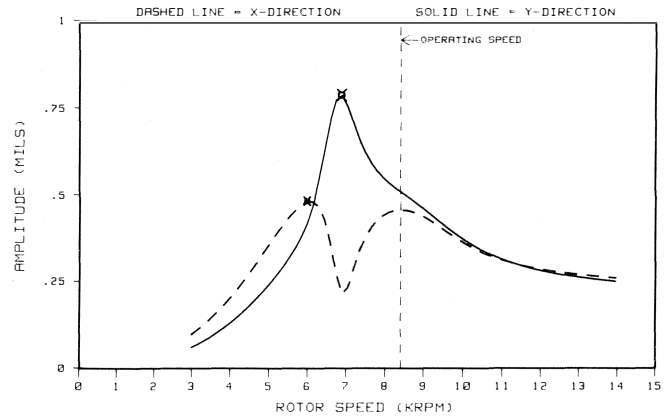

Figure 31a. Synchronous Response Amplitudes vs Rotor Speed at Second Stage Wheel Location (Near Rotor Center) for Compressor Configuration Number Three—Considers Rotor Supported in Locked, Outer Oil Seal Bushings. Also considers effects of unloaded (centered) tilting pad journal bearings on flexible pedestals (kp = 1 × 10^5 lb/in).
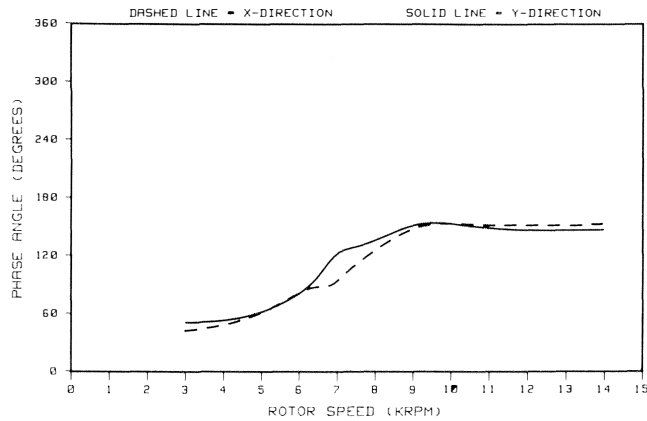

Figure 30b. Response Phase Angles vs Rotor Speed at Thrust-end Bearing Location for Compressor Configuration Number Three.
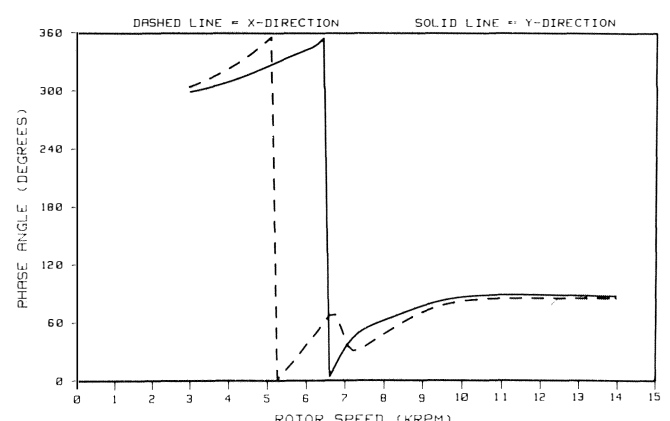

Figure 31b. Response Phase Angles vs Rotor Speed at Second Stage Wheel Location (Near Rotor Center) for Compressor Configuration Number Three.
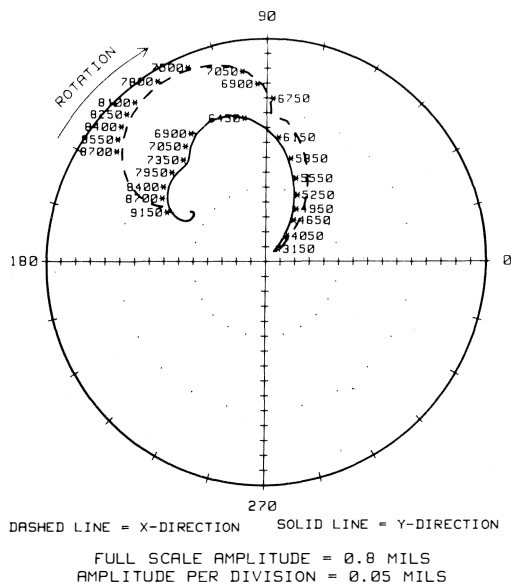

Figure 30c. Nyquist Plot of Response at Thrust-end Bearing Location for Compressor Configuration Number Three.
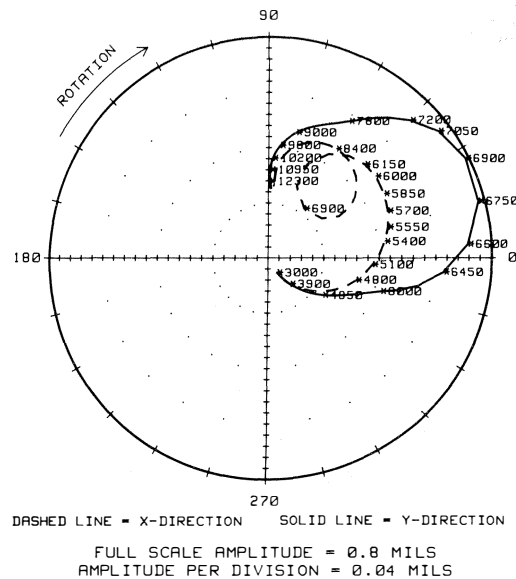

Figure 31c. Nyquist Plot of Response at Second Stage Wheel Location (Near Rotor Center) for Compressor Configuration Number Three.
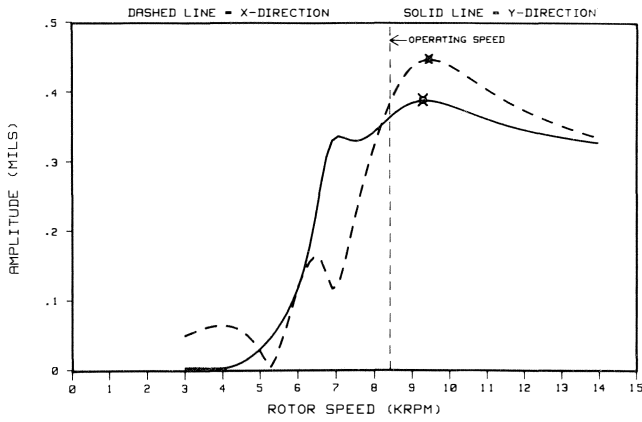
Figure 32a. Synchronous Response Amplitudes at Coupling-end Bearing Location for Compressor Configuration Number Three—Considers Rotor Supported in Locked, Outer Oil Seal Bushings. Also considers effects of unloaded (centered) tilting pad journal bearings on flexible pedestals (Kp = 1 × 10^5 lb/in).

Figure 32b. Response Phase Angles vs Rotor Speed vs Rotor Speed at Coupling-end Bearing Location for Compressor Configuration Number Three.

FULL SCALE AMPLITUDE = 0.5 MILS
AMPLITUDE PER DIVISION = 0.02 MILS

Figure 32c. Nyquist Plot of Response at Coupling-end Bearing Location for Compressor Configuration Number Three.
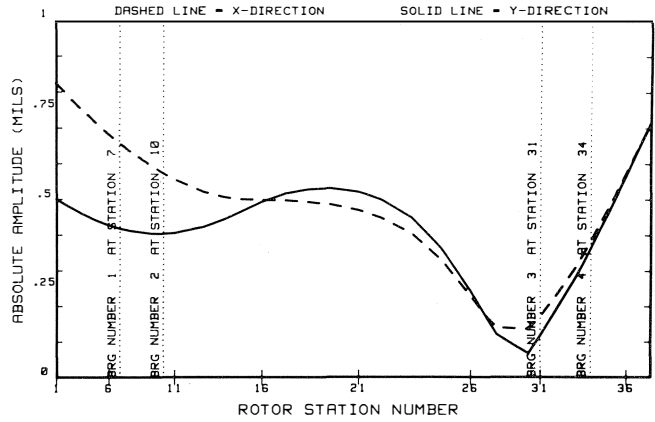

Figure 33. Magnitude of Synchronous Response Amplitude Vectors (Magnitude Only) Along Rotor Shaft at Running Speed (8400 CPM) for Compressor Configuration Number Three.
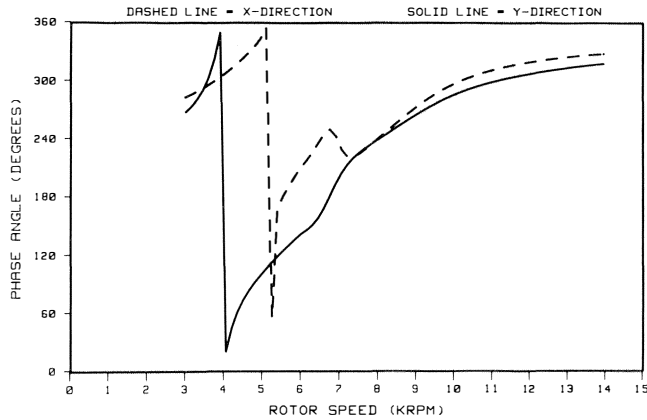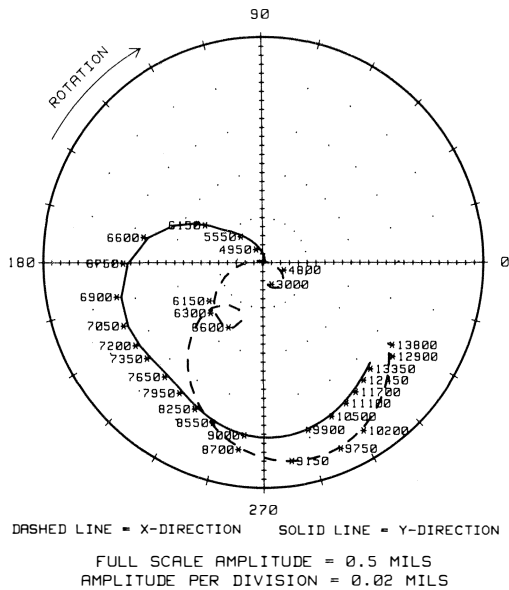
Table 15. Rotor Stability vs. Aerodynamic Cross-coupling for Compressor Supported in Tilting Pad Journal Bearings Only. Oil seal bushing effects not considered.

Beta Value	Aero Q Per Wheel (lb/in)	Total Aero Q 2 Stages (lb/in)	Frequency (cpm)	Log Dec
0	0	0	4,646	+0.9
1	2,537	5,074	4,701	+0.9
2	5,074	10,148	4,723	+0.8
3	7,611	15,222	4,724	+0.7
4	10,148	20,296	4,722	+0.6
8	20,296	40,592	4,716	+0.2

Table 16. Rotor Stability vs. Aerodynamic Cross-coupling for Compressor Supported in Tilting Pad Journal Bearings on Rigid Pedestals. Locked, unloaded (centered) outer oil seal bushing effects included.

Beta Value	Aero Q Per Wheel (lb/in)	Total Aero Q 2 Stages (lb/in)	Frequency (cpm)	Log Dec
0	0	0	5,024	+0.9
1	2,537	5,074	5,024	+0.8
2	5,074	10,148	5,027	+0.7
3	7,611	15,222	5,032	+0.6
4	10,148	20,296	5,038	+0.5
8	20,296	40,592	5,083	+0.11

Locked Seals Carry Rotor—
Unloaded Bearings on Rigid Pedestals

The rotor stability, assuming locked outer oil seal bushings support the rotor, is listed in Table 17. In addition, it is assumed that the tilt pad bearings are unloaded. The bearing pedestals are assumed to be rigid. With no aerodynamic cross-coupling, the logarithmic decrement is +0.7. If an aerodynamic load of 40592 lb/in is considered, the rotor would be marginally stable (with a logarithmic decrement of +0.01).

Table 17. Rotor Stability vs. Aerodynamic Cross-coupling for Compressor Supported in Locked, Outer Oil Seal Bushings. Also considers effects of unloaded (centered) tilting pad journal bearings on rigid pedestals.

Beta Value	Aero Q Per Wheel (lb/in)	Total Aero Q 2 Stages (lb/in)	Frequency (cpm)	Log Dec
0	0	0	5,190	+ 0.7
1	2,537	5,074	5,190	+ 0.6
2	5,074	10,148	5,196	+ 0.5
3	7,611	15,222	5,204	+ 0.5
4	10,148	20,296	5,213	+ 0.4
8	20,296	40,592	5,263	+ 0.01

Locked Seals Carry Rotor—
Unloaded Bearings on Flexible Pedestals

The rotor stability results, assuming locked outer oil seal bushings support the rotor, are listed in Table 18. In this case, it is also assumed that the tilt pad bearings are unloaded, but the bearing pedestals are considered to be flexible, with stiffnesses of 1×10^5 lb/in. In this case, the system is unstable under all conditions. With no aerodynamic cross-coupling, the logarithmic decrement is -0.13. For an aerodynamic cross-coupling value of 40592 lb/in, the logarithmic decrement is -0.5.

Table 18. Rotor Stability vs. Aerodynamic Cross-coupling for Compressor Supported in Locked, Outer Oil Seal Bushings. Also considers effects of unloaded (centered) tilting pad journal bearings on flexible pedestals ($Kp = 1x10^5$).

Beta Value	Aero Q Per Wheel (lb/in)	Total Aero Q 2 Stages (lb/in)	Frequency (cpm)	Log Dec
0	0	0	4,005	− 0.13
1	2,537	5,074	4,035	− 0.18
2	5,074	10,148	4,067	− 0.24
3	7,611	15,222	4,099	− 0.29
4	10,148	20,296	4,131	− 0.34
8	20,296	40,592	4,267	− 0.5

In summary, the present rotor/bearing system on rigid bearing pedestals is stable, with or without seal effects, for aerodynamic cross-coupling as high as 20000 lb/in. This corresponds to a beta value of four, which is considered a very high value for most turbomachinery. In general, the seal effects decrease system stability. Stability is highest with no seals, and lowest with the seals carrying all of the load. If bearing pedestal flexibility is introduced, the system is unstable.

EVALUATION OF RADIAL BEARING RETAINER FITS

One normally considers the bearing supports on a barrel compressor to be very rigid, because the bearings are usually tucked into the end head of the casing. However, in this case, the bearings are "breach-mounted" into the case and axially bolted through the retainers against a vertical face.

In order to physically install these bearing retainers, there has to be some clearance between the retainer outside diameter and the bore of the mating part. Clearances of 0.5 mils to 2.2 mils on the thrust end are indicated in Table 19. Clearances of 1.0 mils to 2.7 mils on the coupling end are indicated in Table 20. There-

Table 19. Bearing Retainer Fit Clearances (Inches) at Thrust-end Bearing.

A. Primary Fit

		Retainer OD	$9.9995 \pm \frac{0.000}{0.0007}$ (inches)
		9.9995	9.9988
Mating Bore $10.000 \pm \frac{0.001}{0.000}$	10.000	0.0005	0.0012
	10.001	0.0015	0.0022
(Inches)			

B. Secondary Fit

		Retainer OD	$9.873 \pm \frac{0.000}{0.001}$ (inches)
		9.873	9.872
Mating Bore $9.875 \pm \frac{0.001}{0.001}$	9.876	0.003	0.004
	9.874	0.001	0.002
(Inches)			

Table 20. Bearing Retainer Fit Clearances (Inches) at Coupling-end Bearing.

		Retainer OD	$11.2490 \pm \frac{.0}{.0007}$ (inches)
		11.2490	11.2483
Mating Bore $11.250 \pm \frac{0.001}{0.000}$	11.251	0.002	0.0027
	11.250	0.001	0.0017
(Inches)			

fore, the only real restraint results from friction at the bolted interface. If this restraint mechanism does not hold the bearings tightly (as would be the case if the bolts vibrated loose), the bearing retainer would be loose in the mating bore. This is where the bearing pedestal stiffness modifies the analysis. If the seals lock up and support the rotor, the bearings become unloaded. This "flexible pedestal" model corresponds to configuration 3.

When the bearings are loaded, the bearing retainers are held firmly down in the bore. Therefore, even if the retainers were not fully restrained by the bolting, they would "bottom out." The result is a stiff pedestal support under the bearings. This model would correspond to configuration 1.

A field modification was made on the coupling-end journal bearing in order to minimize the possibility of the bearing retainer becoming loose. Two 3/8 in holes were drilled and tapped radially through the compressor end head plate at 45 degrees off top-dead-center (Figure 34). Dog-point set screws were installed in these holes to restrain the bearing retainer in the event that the axial cap screws became loose. Therefore, this modification would help prevent the radial retainer freedom which introduces the "flexible pedestal" effect, as previously described.

SUMMARY AND CONCLUSIONS

This analysis has shown that the present rotor/bearing system can run as two entirely different systems that correlate well with field observations.

The first system corresponds to the "normal" running condition. In this case, the bearings support all, or most, of the gravitational load. In this case, the seal bushings operate at low
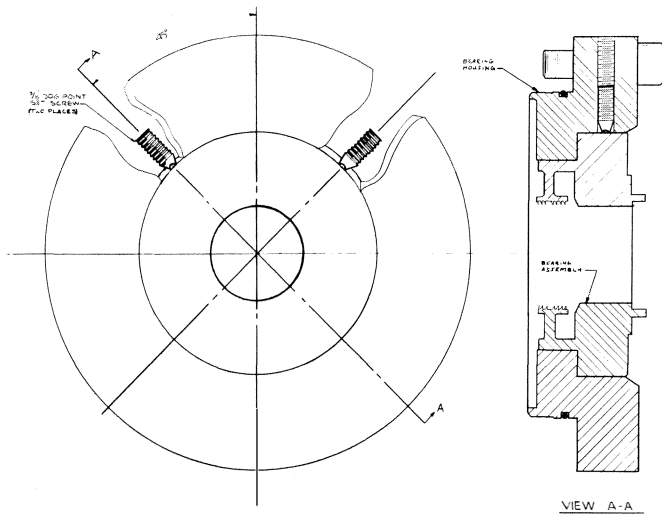
Figure 34. Coupling-end Bearing Modified With Set Screws to Secure Retainer in Bore.

eccentricities, which is similar to the centered condition assumed in this analysis.

The second system corresponds to the condition where there are high vibration levels at the running speed. In this case, the seals carry the rotor weight and unload the bearings. Due to this unloading, a level of flexibility can be introduced under the bearing retainers. Note that in order to meet the assumptions for the second system, two requirements must be met:

• *Seal Bushing Lock Up.* The outer seal bushings must be locked against their vertical sliding faces. The outer seal bushings are subjected to a 1710 psi pressure differential. This can generate a friction force of 1517 lb (2.6 times the rotor weight). Therefore, these bushings can lock up and act similar to plain journal bearings with external pressurization.

• *Flexible Bearing Pedestals.* The tilt pad journal bearing pedestals must become effectively flexible (or loose). This is how the bearing pedestal effective flexibility (looseness) fits into the analysis. If the seals lock up and support the rotor, the bearings become unloaded. This "flexible pedestal" model corresponds to the configuration 3.

When the bearings are loaded, the bearing retainers are held firmly down in the bore. Therefore, even if the retainers were not fully restrained by the bolting, they would 'bottom out." The result is a stiff pedestal support under the bearings. This model would correspond to the configuration 1.

For the first system (with the bearings carrying all of the load, locked centered seals, and rigid bearing pedestals), the peak response speeds are between 5400 cpm and 6000 cpm. The peak response at 5400 cpm correlates well with the first critical speed measured in the field. However, there are no peak responses near the running speed for this case.

For the second system (with locked outer seal bushings carrying all of the load, unloaded tilt pad bearings, and flexible bearing pedestals), there are peak response speeds near the running speed (8400 cpm). These responses correspond to the excitation of the second critical speed. In this mode, the amplitudes at the ends of the rotor are high relative to the rest of the shaft. Therefore, in this condition, the rotor is very sensitive to unbalance at the thrust collar and coupling.

The stability analysis showed that the present rotor-bearing system is very stable with or without seal effects for aerodynamic cross-coupling values as high as 20000 lb/in. This corresponds to a "beta value" of four, which is considered a very high value for most turbomachinery [8]. The stability is highest with no seals. The stability is reduced if the seals carry the entire rotor. For 40592 lb/in of aerodynamic cross-coupling load, the system is marginally stable. This corresponds to a beta value of eight. When bearing pedestal flexibility is introduced under the unloaded bearings, the logarithmic decrements indicate an unstable system.

Therefore, this analysis has demonstrated that the recycle gas compressor bearings must be rigidly supported at all times in order to maintain vibration control. To this end, the coupling-end bearing retainer was modified with additional restraining set screws. The purpose of this modification was to minimize the chance for bearing radial looseness, which can introduce effective pedestal flexibility when the bearings become unloaded. Subsequent to this modification, the compressor ran for three years without failure.

REFERENCES

1. Salamone, D. J., "Journal Bearing Design Types and Their Applications to Turbomachinery," *Proceedings of the Thirteenth Turbomachinery Symposium*, Turbomachinerry Laboratories, Department of Mechanical Engineering, Texas A&M University, College Station, Texas, pp. 179-188 (1984).

2. Barrett, L. E., Gunter, E. J. and Allaire, P. E. "Optimum Bearing and Support Damping for Unbalance Response and Stability of Rotating Machinery," Journal of Engineering for Power, Transactions of ASME, *100* (1), pp. 89-94 (1978).

3. Salamone, D. J., "Introduction to Hydrodynamic Journal Bearings," *Vibration Institute Minicourse Notes— Machinery Vibration Monitoring and Analysis*, Clarendon Hills, Illinois: The Vibration Institute, pp. 41-56 (1985).

4. Lund, J. W. and Orcutt, F. K., "Calculations and Experiments on the Unbalance Response of a Flexible Rotor," Journal of Engineering for Industry, Transactions of ASME (November 1967).

5. Salamone, D. J. and Gunter, D. J., "Effects of Shaft Warp and Disk Skew on the Synchronous Unbalance Response of a Multimass Flexible Rotor in Fluid Film Bearings," *Topics in Fluid Film Bearing and Rotor Bearing System Design and Optimization*, ASME Book No. 100118 (1978).

6. Gunter, E. J., "Dynamic Stability of Rotor-Bearing Systems," NASA SP-113 (1966).

7. Lund, J. W., "Stability and Damped Critical Speeds of a Flexible Rotor in Fluid Film Bearings," Journal of Engineering for Industry, Transactions of ASME, pp. 509-517 (May 1974).

8. Alford, J. S., "Protecting Turbomachinery from Self Excited Rotor Whirl," Journal of Engineering for Power, Transactions of ASME, pp. 333-344 (October 1965).

ACKNOWLEDGEMENT